LABORATORI NAZIONALI DI FRASCATI
SIS-Pubblicazioni

LNF-98/003(P)
29 Gennaio 1998

CERN-TH/97-374
hep-ph/9801456

Nonperturbative Effects in $\bar{B} \to X_s l^+ l^-$ for Large Dilepton Invariant Mass

G. Buchalla[1] and G. Isidori[2]

[1)] *Theory Division, CERN, CH-1211 Geneva 23, Switzerland*

[2)] *INFN, Laboratori Nazionali di Frascati, P.O. Box 13, I-00044 Frascati, Italy*

Abstract

We reconsider the calculation of $\mathcal{O}(\Lambda^2_{QCD}/m_b^2)$ nonperturbative corrections to $\bar{B} \to X_s l^+ l^-$ decay. Our analysis confirms the results of Ali et al. for the dilepton invariant mass spectrum, which were in disagreement with an earlier publication, and for the lepton forward-backward asymmetry. We also give expressions for the $\mathcal{O}(\Lambda^2_{QCD}/m_b^2)$ corrections to the left-right asymmetry. In addition we discuss the breakdown of the heavy quark expansion near the point of maximal dilepton invariant mass q^2 and consider a model independent approach to this region using heavy hadron chiral perturbation theory. The modes $\bar{B} \to \bar{K} l^+ l^-$ and $\bar{B} \to \bar{K}\pi l^+ l^-$, which determine the endpoint region of the inclusive decay, are analysed within this framework. An interpolation is suggested between the region of moderately high q^2, where the heavy quark expansion is still valid, and the vicinity of the endpoint described by chiral perturbation theory. We also comment on further nonperturbative effects in $\bar{B} \to X_s l^+ l^-$.

PACS: 13.20.He,12.39.Hg

Submitted to Nucl. Phys. B

1 Introduction

The inclusive decay $\bar{B} \to X_s l^+ l^-$ ($l = e, \mu, \tau$) has received considerable interest in the literature [1]–[19]. As a loop-induced flavour-changing neutral current (FCNC) process it provides a sensitive probe of flavour dynamics, the least tested sector of the Standard Model. The rare decay modes $\bar{B} \to X_s l^+ l^-$ are well within reach of the next generation of precision B physics experiments and promise to yield much needed information complementary to that from other sources such as $\bar{B} \to X_s \gamma$, $\bar{B} \to X_s \nu \bar{\nu}$, $B - \bar{B}$ mixing, CP violation or rare K decays. The interest in $\bar{B} \to X_s l^+ l^-$ and other inclusive rare B decay processes is reinforced by the fact that their theoretical treatment is fairly well under control. Indeed, the rate for $\bar{B} \to X_s l^+ l^-$ is dominated, in the region of $q^2 = (p_{l^-} + p_{l^+})^2$ away from resonance backgrounds, by perturbatively calculable contributions. These are known at next-to-leading order (NLO) [7,8]. Such a calculation at the parton level is formally justified by the heavy quark expansion (HQE), in which the free b quark decay $b \to s l^+ l^-$ emerges as the leading contribution to $\bar{B} \to X_s l^+ l^-$. This result receives power corrections of the form $(\Lambda_{QCD}/m_b)^n$, which can be systematically addressed within the HQE framework. The leading corrections arise at order $n = 2$. They have been first considered in [5]. A further computation of these effects in [14] did not confirm the results obtained in [5]. In particular, in [14] the relative $\mathcal{O}(\Lambda^2_{QCD}/m_b^2)$ correction diverges at the high-q^2 endpoint, indicating a manifest breakdown of the heavy quark expansion, a feature that is absent in [5].

The $\mathcal{O}(\Lambda^2_{QCD}/m_b^2)$ effects are relevant both conceptually, for assessing the validity of the HQE, as well as for obtaining quantitative control over a class of theoretical uncertainties beyond perturbation theory. In view of this, the phenomenological interest of $\bar{B} \to X_s l^+ l^-$ and the situation in the literature described above, a further independent analysis of the issue is certainly useful. The results of such an analysis of the $\mathcal{O}(\Lambda^2_{QCD}/m_b^2)$ corrections in $\bar{B} \to X_s l^+ l^-$ will be presented in this paper. We will furthermore discuss the breakdown of the HQE near the endpoint of the spectrum (at maximum q^2). The implications of this feature for a description of the high-q^2 region will be pointed out. A major part of this work will then be devoted to investigating the model independent constraints on the q^2-spectrum that can be obtained using heavy hadron chiral perturbation theory (HHChPT).

The paper is organized as follows. A brief description of the general framework and a collection of basic formulas is given in Section 2. In Section 3 we present our results for the $1/m_b^2$ corrections to the dilepton invariant mass spectrum, the forward-backward (FB) asymmetry and the left-right (LR) asymmetry in $\bar{B} \to X_s l^+ l^-$. Section 4 contains a discussion of the breakdown of the HQE near the endpoint. In this section we also analyze

the endpoint region of $\bar{B} \to X_s l^+ l^-$ in terms of the exclusive modes $\bar{B} \to \bar{K} l^+ l^-$ and $\bar{B} \to \bar{K}\pi l^+ l^-$, calculated within chiral perturbation theory. A few comments on further nonperturbative effects in $\bar{B} \to X_s l^+ l^-$ are made in Section 5. We summarize our results in Section 6.

2 Framework and Basic Expressions

The starting point for the analysis of $\bar{B} \to X_s l^+ l^-$ is the effective Hamiltonian, in the Standard Model given by (neglecting the small contribution $\sim V_{us}^* V_{ub}$)

$$\mathcal{H}_{eff} = -\frac{G_F}{\sqrt{2}} V_{ts}^* V_{tb} \left[\sum_{i=1}^{8} C_i(\mu) Q_i + \frac{\alpha}{2\pi} \tilde{C}_9(\mu) (\bar{s}b)_{V-A} (\bar{l}l)_V + \frac{\alpha}{2\pi} \tilde{C}_{10} (\bar{s}b)_{V-A} (\bar{l}l)_A \right] . \tag{1}$$

The Hamiltonian is known at next-to-leading order [7,8]. A detailed review may be found in [20], where the Wilson coefficients C_i and the four-quark operators Q_i are defined explicitly (the operators are typically of the form $Q_i \sim (\bar{s}b)(\bar{c}c)$, for $i = 1, \ldots, 6$, whereas $Q_7 \sim e m_b \bar{s} \sigma^{\mu\nu} (1+\gamma_5) b F_{\mu\nu}$ and $Q_8 \sim g m_b \bar{s} \sigma^{\mu\nu} (1+\gamma_5) \lambda^a b G^a_{\mu\nu}$).
From (1) the following general expression can be derived for the differential decay rate

$$\begin{aligned} \frac{d\Gamma(\bar{B} \to X_s l^+ l^-)}{dx\, dy\, ds} &= \frac{G_F^2 m_b^5}{192\pi^3} |V_{ts}^* V_{tb}|^2 \frac{\alpha^2}{4\pi^2} \frac{3}{4\pi m_b^2} \frac{m_b}{M_B} \times \\ &\times \Big[L^S_{\mu\nu} \Big\{ \Big(|\tilde{C}_9^{eff}|^2 + |\tilde{C}_{10}|^2 \Big)\, W_9^{\mu\nu} + 4 m_b^2 |C_7|^2\, W_7^{\mu\nu} + 4 m_b \mathrm{Re}\, C_7 \tilde{C}_9^{eff *}\, W_{97}^{\mu\nu} \Big\} \\ &+ L^A_{\mu\nu} \Big\{ 2\mathrm{Re}\, \tilde{C}_9^{eff *} \tilde{C}_{10}\, W_9^{\mu\nu} + 4 m_b \mathrm{Re}\, C_7 \tilde{C}_{10}^*\, W_{97}^{\mu\nu} \Big\} \Big] . \end{aligned} \tag{2}$$

Here m_b (M_B) is the b-quark (B meson) mass. $\tilde{C}_9^{eff}$ is a (scheme invariant) effective Wilson coefficient that includes, in addition to $\tilde{C}_9$ from (1), the contributions from the $b \to s l^+ l^-$ transition matrix elements of 4-quark operators Q_1, ..., Q_6. Next

$$L^S_{\mu\nu} = p_{1\mu} p_{2\nu} + p_{2\mu} p_{1\nu} - g_{\mu\nu} p_1 \cdot p_2 \qquad \text{and} \qquad L^A_{\mu\nu} = -i \varepsilon_{\mu\nu\varrho\sigma} p_1^\varrho p_2^\sigma \tag{3}$$

are the symmetric and antisymmetric leptonic tensors, respectively (p_1 (p_2) is the momentum of l^- (l^+) and $\varepsilon^{0123} = +1$). We also set $s = q^2/m_b^2$ ($q = p_1 + p_2$), $x = 2p \cdot p_1 / m_b^2$ and $y = 2p \cdot p_2 / m_b^2$, where p is the b-quark momentum defined as $p^\mu = m_b v^\mu$ in terms of the B-meson four-velocity $v^\mu = p_B^\mu / M_B$. The hadronic tensors $W_i^{\mu\nu}$ can be written as $W_i^{\mu\nu} = 2\mathrm{Im}\, T_i^{\mu\nu}$ where

$$T_9^{\mu\nu} = i \int d^4x\, e^{-iq\cdot x} \langle B | T\, j_9^{\dagger\mu}(x) j_9^\nu(0) | B \rangle , \tag{4}$$

$$T_{97}^{\mu\nu} = i \int d^4x\, e^{-iq\cdot x} \langle B | T\, j_9^{\dagger\mu}(x) j_7^{\lambda\nu}(0) | B \rangle \frac{i q_\lambda}{q^2} , \tag{5}$$

$$T_7^{\mu\nu} = i \int d^4x\, e^{-iq\cdot x} \langle B | T\, j_7^{\dagger\lambda\mu}(x) j_7^{\varrho\nu}(0) | B \rangle \frac{q_\lambda q_\varrho}{q^4} , \tag{6}$$

$$j_9^\mu = \bar{s}\gamma^\mu(1-\gamma_5)b\;, \qquad j_7^{\mu\nu} = \bar{s}\sigma^{\mu\nu}(1+\gamma_5)b\;. \tag{7}$$

Here the B meson state $|B\rangle$ is taken in conventional relativistic normalization $\langle B|B\rangle = 2EV$ (the explicit appearance of the factor $1/M_B$ in (2) is due to this definition).
Evaluating the hadronic tensors to leading order in the heavy quark expansion, eq. (2) reproduces the well known quark-level results for the $\bar{B} \to X_s l^+ l^-$ decay distributions and asymmetries. For instance, defining

$$R(s) = \frac{\frac{d}{ds}\Gamma(\bar{B}\to X_s l^+ l^-)}{\Gamma(\bar{B}\to X_c e\nu)}\;, \tag{8}$$

one obtains upon integrating over x and y

$$\begin{aligned} R(s) &= \frac{\alpha^2}{4\pi^2}\left|\frac{V_{ts}}{V_{cb}}\right|^2 \frac{(1-s)^2}{f(z)\kappa(z)} \times \\ &\quad \times\left[(1+2s)\left(|\tilde{C}_9^{eff}|^2+|\tilde{C}_{10}|^2\right)+4\left(1+\frac{2}{s}\right)|C_7|^2+12C_7\mathrm{Re}\tilde{C}_9^{eff}\right]\;. \end{aligned} \tag{9}$$

Here $f(z) = 1-8z^2+8z^6-z^8-24z^4\ln z$ is the phase space factor and $\kappa(z)$ the QCD correction factor ($z = m_c/m_b$) entering $\Gamma(\bar{B}\to X_c e\nu)$; $\kappa(z)$ can be found in [20]. Note that for the dilepton invariant mass spectrum $R(s)$ only the symmetric part in (2) (proportional to $L^S_{\mu\nu}$) contributes. In (9) we have neglected $\mathcal{O}(m_l^2/m_b^2)$ and $\mathcal{O}(m_s^2/m_b^2)$ terms, as we shall do throughout this paper, unless stated otherwise. The expressions given are therefore applicable to the cases $l = e, \mu$. The extensions of (9) to the case $m_l \neq 0$ (relevant for $l = \tau$) and $m_s \neq 0$ are given in [9,12]. Neglecting the strange quark mass is a very good approximation except near the q^2 endpoint. This region, however, suffers from large nonperturbative corrections and the entire partonic approach has to be reconsidered there (we will come back later to this point).

A quantity closely related to $R(s)$ is the left-right (LR) asymmetry, which measures the difference in the rates of producing left handed or right handed leptons in $\bar{B}\to X_s l^+ l^-$ decay. As discussed in [21,22], the LR asymmetry can be directly extracted from (9). Defining

$$R^{L,R}(s) = R(s)\Big|_{\tilde{C}_9^{eff}\to\frac{\tilde{C}_9^{eff}\mp\tilde{C}_{10}}{2},\ \tilde{C}_{10}\to\frac{\tilde{C}_{10}\mp\tilde{C}_9^{eff}}{2},\ |C_7|^2\to\frac{1}{2}|C_7|^2} \tag{10}$$

one has

$$\begin{aligned} A_{LR}(s) &\equiv R^L(s) - R^R(s) \\ &= \frac{\alpha^2}{4\pi^2}\left|\frac{V_{ts}}{V_{cb}}\right|^2 \frac{(1-s)^2}{f(z)\kappa(z)}\left[(1+2s)\left(-2\tilde{C}_{10}\,\mathrm{Re}\,\tilde{C}_9^{eff}\right)-12C_7\tilde{C}_{10}\right]\;. \end{aligned} \tag{11}$$

Another interesting observable that can be studied in $\bar{B} \to X_s l^+ l^-$ decays is the forward-backward (FB) lepton asymmetry [4], which can be defined as

$$A_{FB}(s) = \frac{1}{\Gamma(\bar{B} \to X_c e \nu)} \int_{-1}^{1} d\cos\theta \, \frac{d^2\Gamma(\bar{B} \to X_s l^+ l^-)}{ds \; d\cos\theta} \text{sgn}(\cos\theta) \; , \tag{12}$$

where θ is the angle between l^+ and B momenta in the dilepton center–of–mass frame. As shown in [14] $A_{FB}(s)$ is identical to the energy asymmetry introduced in [11]. The NLO perturbative result for $A_{FB}(s)$ is given by

$$A_{FB}(s) = -\frac{3\alpha^2}{4\pi^2} \left|\frac{V_{ts}}{V_{cb}}\right|^2 \frac{(1-s)^2}{f(z)\kappa(z)} \text{Re}\left\{\tilde{C}_{10}^* \left[2\, C_7 + s\, \tilde{C}_9^{eff}\right]\right\} \; . \tag{13}$$

Interestingly enough, both $A_{LR}(s)$ and $A_{FB}(s)$ are sensitive to the relative signs between C_7, $\tilde{C}_9^{eff}$ and $\tilde{C}_{10}$. These asymmetries therefore offer useful additional information on the underlying short distance physics.

3 $\mathcal{O}(\Lambda_{QCD}^2/m_b^2)$ Power Corrections to R, A_{LR} and A_{FB}

The hadronic tensors $W_i^{\mu\nu}$ in (2) can be systematically expanded in inverse powers of the heavy quark mass using the operator product expansion (HQE) approach supplemented by heavy quark effective theory (HQET). The general procedure is described in great detail in [23] for the case of $\bar{B} \to X_{u,c} l \nu$ decay. The first corrections to the parton result ($\mathcal{O}(1)$) appear at $\mathcal{O}(\Lambda_{QCD}^2/m_b^2)$. To this order we obtain the following expressions for the hadronic tensors (after contracting with $L_{\mu\nu}^S$)

$$\begin{aligned}
\frac{3}{4\pi m_b M_B} \int dx dy \; L_{\mu\nu}^S W_9^{\mu\nu} &= \left(1 + \frac{\lambda_1}{2m_b^2}\right)(1-s)^2(1+2s) \\
&\quad + \frac{3\lambda_2}{2m_b^2}(1 - 15s^2 + 10s^3) \; , \qquad (14) \\
\frac{1}{4\pi M_B} \int dx dy \; L_{\mu\nu}^S W_{97}^{\mu\nu} &= \left(1 + \frac{\lambda_1}{2m_b^2}\right)(1-s)^2 \\
&\quad - \frac{\lambda_2}{2m_b^2}(5 + 6s - 7s^2) \; , \qquad (15) \\
\frac{3m_b}{4\pi M_B} \int dx dy \; L_{\mu\nu}^S W_7^{\mu\nu} &= \left(1 + \frac{\lambda_1}{2m_b^2}\right)(1-s)^2 \left(1 + \frac{2}{s}\right) \\
&\quad - \frac{3\lambda_2}{2m_b^2} \frac{6 + 3s - 5s^3}{s} \; . \qquad (16)
\end{aligned}$$

Here

$$\lambda_1 = \frac{\langle B|\bar{h}(iD)^2 h|B\rangle}{2M_B} \; , \qquad \lambda_2 = \frac{1}{6}\frac{\langle B|\bar{h} g\sigma \cdot G h|B\rangle}{2M_B} = \frac{M_{B^*}^2 - M_B^2}{4} \; , \tag{17}$$

with h the b-quark field in HQET.

The results in (14)–(16) agree with [14] but differ from the findings of [5]. The contribution involving $W_9^{\mu\nu}$ is the same that appears in the case of semileptonic $\bar{B} \to X_u l\nu$ decay. Integration of (14) over s yields $(1/2)[1+(\lambda_1-9\lambda_2)/(2m_b^2)]$, reproducing the well known correction factor derived in [23,24]. Inserting (14)–(16) into (2) we obtain for the $1/m_b^2$ corrections to $R(s)$ in (9)

$$\delta_{1/m_b^2} R(s) = \frac{3\lambda_2}{2m_b^2}\left(\frac{\alpha^2}{4\pi^2}\left|\frac{V_{ts}}{V_{cb}}\right|^2 \frac{1}{f(z)\kappa(z)}\left[(1-15s^2+10s^3)(|\tilde{C}_9^{eff}|^2+|\tilde{C}_{10}|^2)\right.\right.$$

$$\left.\left. -(6+3s-5s^3)\frac{4|C_7|^2}{s} - (5+6s-7s^2)4C_7 \mathrm{Re}\tilde{C}_9^{eff}\right] + \frac{g(z)}{f(z)}R(s)\right) . \qquad (18)$$

Here we have used the normalizing semileptonic rate including terms of order $1/m_b^2$

$$\Gamma(\bar{B}\to X_c e\nu) = \frac{G_F^2 m_b^5}{192\pi^3}|V_{cb}|^2 f(z)\kappa(z)\left[1+\frac{\lambda_1}{2m_b^2} - \frac{3\lambda_2}{2m_b^2}\frac{g(z)}{f(z)}\right] , \qquad (19)$$

$$g(z) = 3-8z^2+24z^4-24z^6+5z^8+24z^4\ln z , \qquad (20)$$

that can be found for instance in [23]. Note that the correction due to the kinetic energy of the b-quark $\sim \lambda_1$ is given as a simple overall factor $(1+\lambda_1/(2m_b^2))$ for both $\bar{B}\to X_c e\nu$ and $\bar{B}\to X_s l^+l^-$ and therefore drops out in the ratio $R(s)$. Since, in contrast to λ_2, the quantity λ_1 is not well known anyway, its absence in (18) is a welcome feature.
Given the results in (14)–(16) it is straightforward to write down the $1/m_b^2$ correction for $A_{LR}(s)$ in (11)

$$\delta_{1/m_b^2} A_{LR}(s) = \frac{3\lambda_2}{2m_b^2}\left(\frac{\alpha^2}{4\pi^2}\left|\frac{V_{ts}}{V_{cb}}\right|^2 \frac{1}{f(z)\kappa(z)}\left[(1-15s^2+10s^3)(-2\tilde{C}_{10}\,\mathrm{Re}\tilde{C}_9^{eff})\right.\right.$$

$$\left.\left. +(5+6s-7s^2)4C_7\tilde{C}_{10}\right] + \frac{g(z)}{f(z)}A_{LR}(s)\right) . \qquad (21)$$

This correction has been discussed previously in [21], however based on the incorrect results of [5].
To calculate the FB asymmetry it is necessary to contract $W_9^{\mu\nu}$ and $W_{97}^{\mu\nu}$ with the asymmetric component of the leptonic tensor. The relevant terms, expanded up to $\mathcal{O}(\Lambda_{QCD}^2/m_b^2)$, are given by

$$\frac{1}{2\pi m_b M_B}\int dxdy\ \mathrm{sgn}(y-x)\ L^A_{\mu\nu}W_9^{\mu\nu} = s(1-s)^2 + \frac{\lambda_1}{6m_b^2}s(3+2s+3s^2)$$

$$-\frac{\lambda_2}{2m_b^2}s(9+14s-15s^2) , \qquad (22)$$

$$\frac{1}{2\pi M_B}\int dxdy\ \text{sgn}(y-x)\ L^A_{\mu\nu}W^{\mu\nu}_{97} \;=\; (1-s)^2+\frac{\lambda_1}{6m_b^2}(3+2s+3s^2) \\ -\frac{\lambda_2}{2m_b^2}(7+10s-9s^2)\,, \qquad (23)$$

leading to

$$\delta_{1/m_b^2}A_{FB}(s)=\frac{3\lambda_2}{2m_b^2}\left(\frac{\alpha^2}{4\pi^2}\left|\frac{V_{ts}}{V_{cb}}\right|^2\frac{1}{f(z)\kappa(z)}\text{Re}\left\{\tilde{C}_{10}^*\left[s(9+14s-15s^2)\tilde{C}_9^{eff}\right.\right.\right. \\ \left.\left.\left.+(7+10s-9s^2)2C_7\right]\right\}+\frac{g(z)}{f(z)}A_{FB}(s)\right)+\frac{4\lambda_1}{3m_b^2}\frac{s}{(1-s)^2}A_{FB}(s)\,. \qquad (24)$$

Also in this case our finding is in agreement with [14].

4 The High-q^2 Region

4.1 Generalities

The size of the $\mathcal{O}(\Lambda^2_{QCD}/m_b^2)$ corrections in (18), (21) and (24) is quite moderate, at the level of several percent, for values of s below about 0.6. On the other hand, when s approaches the endpoint ($s=1$), the corrections for R, A_{LR} and A_{FB} tend towards a nonzero value, while the leading term of these quantities vanishes as $(1-s)^2$. The relative correction thus diverges in the limit $s\to 1$ and the rate $R(s)$ becomes even negative for s close enough to the endpoint. Obviously, the HQE breaks down in the endpoint region. From the expressions given above one may recognize that in the case of $R(s)$ and A_{LR} this behaviour is exclusively related to the λ_2-term, whereas in the case of A_{FB} also the kinetic energy correction $\sim\lambda_1$ is not well behaved in the limit $s\to 1$. We remark that these features are not shared by the result given in [5] and have been first observed by the authors of [14].

In order to account for nonperturbative effects that elude the HQE approach, [14] supplement the partonic calculation with a Fermi-motion model to predict the q^2 spectrum and the shape of the FB asymmetry in the entire physical region including the endpoint. Although such an approach could be useful in principle, in particular when employed in conjunction with experimental data (used e.g. to fit model parameters), we will not perform such an analysis here. Instead, we would like to discuss to what extent model independent predictions can be made for the $\bar{B}\to X_s l^+l^-$ spectrum. We will thereby focus our attention on the high-q^2 region. For this purpose we shall first discuss the nature of the breakdown of HQE in slightly more detail. We follow here the general discussion presented in [25,26].

The central element in the operator product expansion of the tensors $T_i^{\mu\nu}$ in (4) is the s-quark propagator. This propagator emerges in the evaluation of the time-ordered products (4) and determines essential features of the $1/m_b$ expansion. Denoting $k=m_b v-q$,

$D_\mu = \partial_\mu - igA_\mu$ and neglecting the s-quark mass, the s-quark propagator in a gluon background field may be written as

$$S_s(k) = \frac{\not{k} + i\,\not{D}}{k^2 + 2ik\cdot D - \not{D}\,\not{D} + i\varepsilon}\,. \tag{25}$$

Up to terms of order $\Lambda_{QCD} \equiv \Lambda$, k is the momentum of the final state hadronic system. In the usual case, that is away from singular kinematical points, one has $k \sim m_b$, $k^2 \sim m_b^2$ and consequently the hierarchy $k^2 \sim m_b^2 \gg k\cdot D \sim m_b\Lambda \gg \not{D}\;\not{D} \sim \Lambda^2$. Therefore one can expand $S_s(k) = \not{k}/k^2 + \mathcal{O}(\Lambda/m_b)$ and the usual HQE is valid.
A different situation arises in the endpoint region of the lepton energy spectrum in $\bar{B} \to X_{c,u} l\nu$ and for the photon energy spectrum in $\bar{B} \to X_s\gamma$. Here one still has $k \sim m_b$ in terms of components, however the kinematics is now such that $k^2 \sim m_b\Lambda$. For the quantities in the denominator of (25) this implies $k^2 \sim m_b\Lambda \approx k\cdot D \sim m_b\Lambda \gg \not{D}\;\not{D} \sim \Lambda^2$. An expansion in Λ/m_b is still possible, but $k\cdot D/k^2$ is now of $\mathcal{O}(1)$ and the corresponding effects have to be resummed to all orders. This is the case discussed in detail in [26,27] for $\bar{B} \to X_{c,u} l\nu$ and in [28] for $\bar{B} \to X_s\gamma$ (see also [25]).
We would like to stress that the situation encountered in the endpoint region of the q^2 spectrum in $\bar{B} \to X_s l^+ l^-$ is substantially different from the two cases just described. For the kinematics that is relevant here, $q^2 \approx m_b^2 \approx M_B^2$, it follows that $k \sim \Lambda$ and $k^2 \sim \Lambda^2$. Then all three terms in the denominator of (25) are of the same order of magnitude $\sim \Lambda^2$. The heavy quark expansion breaks down completely and not even an all-orders resummation, of the type useful for $\bar{B} \to X_{c,u} l\nu$ and $\bar{B} \to X_s\gamma$, can be performed. This conclusion is clear on physical grounds, since at $q^2 \approx M_B^2$ the two leptons are emerging back-to-back, carrying almost all the energy released in the decay of the B meson. The final state hadronic system has very low momentum and we are in a regime of manifestly nonperturbative QCD.

At this point we would like to emphasize a conceptual consequence of this discussion for the treatment of the q^2 spectrum in $\bar{B} \to X_s l^+ l^-$ within a Fermi-motion model, as employed in [14]. In the case of the photon energy spectrum in $\bar{B} \to X_s\gamma$ or the lepton energy spectrum in $\bar{B} \to X_{c,u} l\nu$ the resummation of leading singular contributions in the HQE leads to a description of the endpoint region in terms of a shape function [27,28,25]. The shape function depends on nonperturbative physics that can qualitatively, at least to some extent, be modeled by a Gaussian description of the b-quark momentum distribution inside the B meson (Fermi-motion). As explained above, a similar interpretation does not exist in the case of $\bar{B} \to X_s l^+ l^-$. A Fermi-motion description of nonperturbative effects, particularly for high q^2, appears therefore certainly less justified than in the usual applications to $\bar{B} \to X_s\gamma$ and $\bar{B} \to X l\nu$. In fact, as we have seen above, the divergence of the $1/m_b^2$ corrections to the q^2 spectrum near the endpoint arises from the chromomagnetic

interaction term $\sim \lambda_2$ that does not have an obvious interpretation in terms of a Fermi-motion ansatz.

On the other hand, the kinematical situation in $\bar{B} \to X_s l^+ l^-$ near the q^2 endpoint, with few, low-momentum hadrons in the final state, lends itself to a treatment using heavy hadron chiral perturbation theory (HHChPT) [29,30]. Combining this description at very high q^2 with the standard HQE result at somewhat lower q^2, where the latter is still valid, a model independent analysis of the entire high-q^2 region (above the Ψ and Ψ' resonances) could be conceived. In the following we shall examine such a possibility.

First, one may write down an effective Hamiltonian, suitable for the endpoint region ($q^2 \to M_B^2$) in $\bar{B} \to X_s l^+ l^-$. This Hamiltonian differs from the standard Hamiltonian (1). 'Light' quark (u, d, s, c) loops may be integrated out explicitly since they involve the hard external scale $q^2 \sim m_b^2 \gg 1GeV$. This endpoint effective Hamiltonian then takes the form, valid at NLO in QCD

$$\mathcal{H}_{eff,EP} = -\frac{G_F}{\sqrt{2}} V_{ts}^* V_{tb} \frac{\alpha}{2\pi} \times \tag{26}$$
$$\times \left[\tilde{C}_{9,EP} (\bar{s}b)_{V-A} (\bar{l}l)_V + \tilde{C}_{10} (\bar{s}b)_{V-A} (\bar{l}l)_A + 2 m_b C_7 \, \bar{s} \sigma^{\mu\nu} (1+\gamma_5) b \frac{i q_\mu}{q^2} \bar{l} \gamma_\nu l \right] .$$

The Wilson coefficient $\tilde{C}_{9,EP}$ has the structure

$$\tilde{C}_{9,EP} = \tilde{C}_9^{NDR} + h(z,s)(3C_1^{(0)} + C_2^{(0)}) + \text{ (penguin contributions)} , \tag{27}$$

with $C_1^{(0)}$, $C_2^{(0)}$, $\tilde{C}_9^{NDR}$ from (1). These quantities, the function $h(z,s)$ and the remaining terms can be found in [20]. $\tilde{C}_{9,EP}$ is identical to $\tilde{C}_9^{eff}$ in (2) (see also [20]), except that it does not include the QCD correction $\tilde{\eta}(s)$ to the matrix element of the current $(\bar{s}b)_{V-A}$, which multiplies $\tilde{C}_9^{NDR}$ in $\tilde{C}_9^{eff}$.

The Hamiltonian (26) is still normalized at a scale $\mu = \mathcal{O}(m_b)$. A further evolution down to hadronic scales ~ 1 GeV is calculable perturbatively using HQET ('hybrid renormalization'). However the HQET logarithms will be automatically contained in the matrix elements of the $(\bar{s}\Gamma b)$ operators if they are taken in full QCD and appropriately normalized at $\mu = \mathcal{O}(m_b)$. It is therefore not necessary to make these effects explicit in (26).

4.2 $\bar{B} \to \bar{K} l^+ l^-$

At the very high end of the spectrum, between the $K\pi$ threshold and the physical endpoint, the inclusive decay $\bar{B} \to X_s l^+ l^-$ degenerates into the exclusive mode $\bar{B} \to \bar{K} l^+ l^-$. Introducing the variable $s_m \equiv q^2/M_B^2$, this region corresponds to $s_m^{K\pi} \le s_m \le s_m^K$ where $s_m^K = s_{m,max} = (1 - M_K/M_B)^2 = 0.821$ and $s_m^{K\pi} = 0.774$.

The matrix elements needed for $\bar{B} \to \bar{K} l^+ l^-$ can be written as

$$\langle \bar{K}(p_{_K})|\bar{s}\gamma_\mu(1-\gamma_5)b|\bar{B}(p)\rangle = f_+(q^2)(p+p_{_K})_\mu + f_-(q^2)(p-p_{_K})_\mu \ , \tag{28}$$

$$\langle \bar{K}(p_{_K})|\bar{s}\sigma^{\mu\nu}b|\bar{B}(p)\rangle = -ia_T(q^2)(p^\mu_{_K}p^\nu - p^\nu_{_K}p^\mu) \ , \tag{29}$$

in terms of the form factors $f_\pm(q^2)$ and $a_T(q^2)$. The decay rate (normalized to the semileptonic width as in (8)) is then given by [31]

$$R_K(s_m) \equiv \frac{\frac{d}{ds_m}B(\bar{B}\to \bar{K}l^+l^-)}{B(\bar{B}\to X_c e\nu)} = \frac{\tau(B_d)}{B(\bar{B}\to X_c e\nu)}\frac{G_F^2 M_B^5}{192\pi^3}|V_{tb}V_{ts}|^2\frac{\alpha^2}{4\pi^2}f_1(s_m)\times$$
$$\times\left\{\frac{f_+^2}{2}\left(|\tilde{C}_{9,EP}|^2+|\tilde{C}_{10}|^2\right)+\frac{a_T^2}{2}m_b^2|C_7|^2 - f_+ a_T m_b \mathrm{Re}\, C_7\tilde{C}^*_{9,EP}\right\} \ , \tag{30}$$

where the phase space function f_1 reads

$$f_1(s_m) = ((1-\varrho+s_m)^2-4s_m)^{3/2} \ , \qquad \varrho = \frac{M_K^2}{M_B^2} \ . \tag{31}$$

In general, the form factors are very difficult to calculate. However, as long as we are interested in high q^2, where the kaon momentum is small, HHChPT may be used to estimate these nonperturbative quantities. In this approach, to the lowest order, one finds [29,30,32,33]

$$f_\pm = -\frac{f_B}{2f_\pi}\left(1 \pm g\frac{M_B \mp v\cdot p_{_K}}{v\cdot p_{_K}+\Delta+\mu_s}\right) \ , \qquad v\cdot p_{_K} = \frac{M_B^2+M_K^2-q^2}{2M_B} \ , \tag{32}$$

$$a_T = \frac{gf_B}{f_\pi}\frac{1}{v\cdot p_{_K}+\Delta+\mu_s} \ . \tag{33}$$

Here f_B and f_π are the B meson and the pion decay constants in the normalization where $f_\pi = 132\,\mathrm{MeV}$. $\Delta = M_{B^*} - M_B = 46\,\mathrm{MeV}$, $\mu_s = M_{B_s} - M_B = 90\,\mathrm{MeV}$ and g is the HHChPT parameter that determines $B^*B\pi$ and $D^*D\pi$ couplings at low energy. The value of g could in principle be inferred from a measurement of $\Gamma(D^* \to D\pi)$, but present data only allow to set an upper limit $g^{exp} < 0.7$. According to the theoretical estimates of [33] in the following we will assume $0.4 < g < 0.6$.

4.3 $\bar{B} \to \bar{K}\pi l^+ l^-$

Between $K\pi$ and $K\pi\pi$ thresholds, i.e. for $s_m^{K\pi\pi} = 0.728 \le s_m \le s_m^{K\pi}$, also the $\bar{B} \to \bar{K}\pi l^+ l^-$ decay is kinematically allowed. No other modes are permitted and the hadronic invariant mass is still small enough to justify the use of HHChPT.

m_b	m_c	$\lvert V_{cb}\rvert$	$\lvert V_{ts}\rvert$	$\lvert V_{tb}\rvert$
4.8 GeV	1.4 GeV	0.04	0.04	1
$\bar{m}_t(m_t)$	M_W	$\sin^2\Theta_W$	α^{-1}	$\Lambda^{(5)}_{\overline{MS}}$
170 GeV	80.2 GeV	0.23	129	0.225 GeV
M_B	M_K	M_π	$\tau(B_d)$	$B(\bar{B}\to X_c e\nu)$
5.28 GeV	0.496 GeV	0.140 GeV	1.6 ps	0.104
g	f_B	f_π	$\Delta = M_{B^*} - M_B$	$\mu_s = M_{B_s} - M_B$
0.5	0.180 GeV	0.132 GeV	0.046 GeV	0.090 GeV

Table 1: Compilation of input parameters (central values).

The matrix element of the left-handed current relevant to $\bar{B}\to\bar{K}\pi l^+l^-$ can be generally decomposed in terms of four independent form factors. Defining

$$\langle \bar{K}^i(p_{_K})\pi^j(p_\pi)|\bar{s}\gamma_\mu(1-\gamma_5)b|\bar{B}(p)\rangle = ic_{ij}\left[ap_{\pi,\mu}+bp_{K,\mu}+cp_\mu-2ih\varepsilon_{\mu\alpha\beta\gamma}p^\alpha p_{_K}^\beta p_\pi^\gamma\right]\,, \tag{34}$$

the lowest order HHChPT results are given by [34]

$$a = \frac{gf_B}{f_\pi^2}\frac{M_B}{v\cdot p_\pi+\Delta}\,, \qquad b=0\,, \tag{35}$$

$$\begin{aligned} c &= \frac{f_B}{2f_\pi^2}\left[1-2g\frac{v\cdot p_\pi}{v\cdot p_\pi+\Delta}-\frac{v\cdot(p_{_K}-p_\pi)}{v\cdot(p_{_K}+p_\pi)+\mu_s}\right.\\ &\qquad \left.-2g^2\frac{p_{_K}\cdot p_\pi - v\cdot p_{_K}\, v\cdot p_\pi}{[v\cdot p_\pi+\Delta][v\cdot(p_{_K}+p_\pi)+\mu_s]}\right], \end{aligned} \tag{36}$$

$$h = \frac{g^2f_B}{2f_\pi^2}\frac{1}{[v\cdot p_\pi+\Delta][v\cdot(p_{_K}+p_\pi)+\Delta+\mu_s]}\,, \tag{37}$$

where $|c_{-+}|^2 = |c_{0-}|^2 = 2|c_{00}|^2 = 2|c_{-0}|^2 = 1$.

We have checked the results (35)–(37), first obtained by the authors of [34], and agree with their findings. In addition we need the corresponding matrix element of the magnetic penguin operator. We obtain, again to leading order in HHChPT

$$\begin{aligned} &\langle \bar{K}^i(p_{_K})\pi^j(p_\pi)|\bar{s}\sigma_{\nu\mu}(1+\gamma_5)b\frac{iq^\nu}{q^2}|\bar{B}(p)\rangle = \\ &\qquad ic_{ij}\left[a'p_{\pi,\mu}+b'p_{K,\mu}+c'p_\mu-2ih'\varepsilon_{\mu\alpha\beta\gamma}p^\alpha p_{_K}^\beta p_\pi^\gamma\right]\,, \end{aligned} \tag{38}$$

$$a' = \frac{gf_BM_B}{f_\pi^2q^2(v\cdot p_\pi+\Delta)}\Big[M_B - v\cdot p_{_K} - v\cdot p_\pi$$

$$+g\frac{v\cdot p_K\, v\cdot(p_K+p_\pi)-p_K\cdot p_\pi-M_K^2}{v\cdot(p_K+p_\pi)+\Delta+\mu_s}\Bigg]\,, \tag{39}$$

$$b' = \frac{g^2 f_B M_B}{f_\pi^2 q^2(v\cdot p_\pi+\Delta)}\frac{p_K\cdot p_\pi+M_\pi^2-v\cdot p_\pi\; v\cdot(p_K+p_\pi)}{v\cdot(p_K+p_\pi)+\Delta+\mu_s}\,, \tag{40}$$

$$c' = -\frac{g f_B}{f_\pi^2 q^2(v\cdot p_\pi+\Delta)}\Bigg[M_B v\cdot p_\pi - M_\pi^2 - p_K\cdot p_\pi + g\frac{p_K\cdot p_\pi\; v\cdot(p_K-p_\pi)-M_K^2 v\cdot p_\pi+M_\pi^2 v\cdot p_K}{v\cdot(p_K+p_\pi)+\Delta+\mu_s}\Bigg]\,, \tag{41}$$

$$h' = \frac{g f_B}{2 f_\pi^2 q^2(v\cdot p_\pi+\Delta)}\left[1+g\frac{M_B-v\cdot p_K-v\cdot p_\pi}{v\cdot(p_K+p_\pi)+\Delta+\mu_s}\right]\,. \tag{42}$$

We proceed to compute the decay rate. The necessary four-body phase space integrations can be performed using the general methods reviewed in [34]. The leading behaviour of the differential $\bar{B}\to\bar{K}\pi l^+l^-$ decay rate as a function of $(s_m^{K\pi}-s_m)$ close to the $K\pi$ threshold may be written down analytically. It gives the correct asymptotic behaviour at threshold and can be used as an approximation to the full result for values of s_m not too far from this point. We find

$$R_{K^-\pi^+}(s_m)\equiv\frac{\frac{d}{ds_m}B(\bar{B}\to K^-\pi^+l^+l^-)}{B(\bar{B}\to X_c e\nu)}=\frac{\tau(B_d)}{B(\bar{B}\to X_c e\nu)}\frac{G_F^2M_B^5}{192\pi^3}|V_{tb}V_{ts}|^2\frac{\alpha^2}{4\pi^2}\times$$

$$\times\frac{1}{32\pi^2}\left\{F_9(s_m)\left(|\tilde{C}_{9,EP}|^2+|\tilde{C}_{10}|^2\right)+4F_7(s_m)|C_7|^2+4F_{97}(s_m)\mathrm{Re}\,C_7\tilde{C}_{9,EP}^*\right\}\,, \tag{43}$$

$$F_9(s_m)=\frac{\pi}{4}\frac{(t_1x_1x_2)^{1/2}}{(1-\sqrt{t_1})^{3/2}}\left[w_1^2+\frac{4x_1x_2}{t_1}(1-\sqrt{t_1})w_2^2\right](s_m^{K\pi}-s_m)^3\,, \tag{44}$$

with $x_1=M_\pi/M_B$, $x_2=M_K/M_B$, $t_1=(x_1+x_2)^2$ and $s_m^{K\pi}=(1-x_1-x_2)^2$. The functions F_7 and F_{97} are obtained from F_9 by replacing $w_i^2\to w_i'^2$ and $w_i^2\to w_iw_i'$, respectively, where

$$w_1=\frac{f_BM_B}{f_\pi^2}\left[\frac{gM_\pi}{M_\pi+\Delta}\left(\frac{M_B}{M_K+M_\pi}-1\right)+\frac{M_\pi+\mu_s/2}{M_K+M_\pi+\mu_s}\right]\,, \tag{45}$$

$$w_2=-\frac{f_BM_B}{2f_\pi^2}\frac{gM_B}{M_\pi+\Delta}\,, \tag{46}$$

$$w_1'=\frac{f_BM_B}{f_\pi^2}\frac{gM_\pi}{M_\pi+\Delta}\frac{m_b}{M_K+M_\pi}\,,\qquad w_2'=-\frac{f_BM_B}{2f_\pi^2}\frac{gM_B}{M_\pi+\Delta}\frac{m_b}{M_B-M_K-M_\pi}\,. \tag{47}$$

Adding the two isospin channels, the total result for the nonresonant $\bar{B}_d(B^-)\to\bar{K}\pi l^+l^-$ rate becomes

$$R_{K\pi}\equiv R_{K^-\pi^+}+R_{\bar{K}^0\pi^0}=R_{\bar{K}^0\pi^-}+R_{K^-\pi^0}=\frac{3}{2}R_{K^-\pi^+}\,. \tag{48}$$

With the explicit expressions for $R_{K\pi}$ at hand, we are in a position to estimate the relative importance of the nonresonant $K\pi$ mode relative to the single K channel in the endpoint region. It is clear that the four-body process $\bar{B} \to \bar{K}\pi l^+ l^-$ is phase space suppressed. This is obvious from (43), which exhibits the typical factor of $\sim 1/(16\pi^2)$. More quantitatively we find that $R_{K\pi}$ amounts to less than 2% of R_K at $s_m = 0.7$ and is still less important for larger s_m. $R_{K\pi}$ is therefore negligible in the entire endpoint region, which is completely dominated by R_K. The asymptotic formula (43) describes the behaviour of $R_{K\pi}$ close to threshold ($s_m = 0.774$). For $s_m = 0.7$ (43) overestimates the full result by about 50%. This is still useful for an order of magnitude estimate.
For s_m below 0.7 a substantial enhancement of the $K\pi$ mode is expected due to the contribution of the K^* resonance. However, for $s_m > 0.73$ we are still far enough from the K^* threshold to safely neglect the $K\pi$ mode with respect to the single kaon channel.

4.4 Discussion

In Fig. 1 we compare the HQE result for $R(s)$ with the HHChPT picture close to the endpoint. For this purpose we rescale the ratio $R(s)$ (9) from quark to physical (hadron) kinematics, replacing

$$R(s) \to \tilde{R}(s_m) \equiv \frac{M_B^2}{m_b^2} R\left(\frac{M_B^2}{m_b^2} s_m\right) = \frac{\frac{d}{ds_m} B(\bar{B} \to X_s l^+ l^-)}{B(\bar{B} \to X_c e \nu)} \,. \tag{49}$$

This representation of the quark level result is furthermore useful since it makes the dependence of the prediction on the b-quark mass explicit. The corresponding uncertainty, which will unavoidably exist in comparing theory with experiment, is illustrated in Fig. 1 for the representative range $m_b = (4.8 \pm 0.1)\mathrm{GeV}$. In this context we recall that m_b here refers to the pole quark mass. In fact, since the NLO QCD calculation for $b \to s l^+ l^-$ is available, the distinction of the pole mass from other mass definitions is already meaningful at first nontrivial (i.e. one-loop) order. The value of m_b is to be determined from some other observable and can then be used as input for $\bar{B} \to X_s l^+ l^-$. In principle the error on m_b can be further reduced in the future. We remark that the dependence of $\tilde{R}(s_m)$ on the renormalization scale μ ($m_b/2 < \mu < m_b$) is less than $\pm 5\%$ in the region $0.5 < s_m < 0.7$.

The $1/m_b^2$ corrections to $\bar{B} \to X_s l^+ l^-$, which are included in Fig. 1, are negative for $s_m > 0.5$, increase with s_m and reach about -20% of the leading result for $s_m = 0.65$. As discussed above, nonperturbative effects that are beyond the control of the HQE become important for still larger values of s_m.

Very close to the endpoint at $s_m = 0.821$ HHChPT offers a complementary approach that may be used to constrain the behaviour of the spectrum from the region of large s_m. An interpolation suggests itself between the regime $s_m < 0.65$, where the HQE is valid,

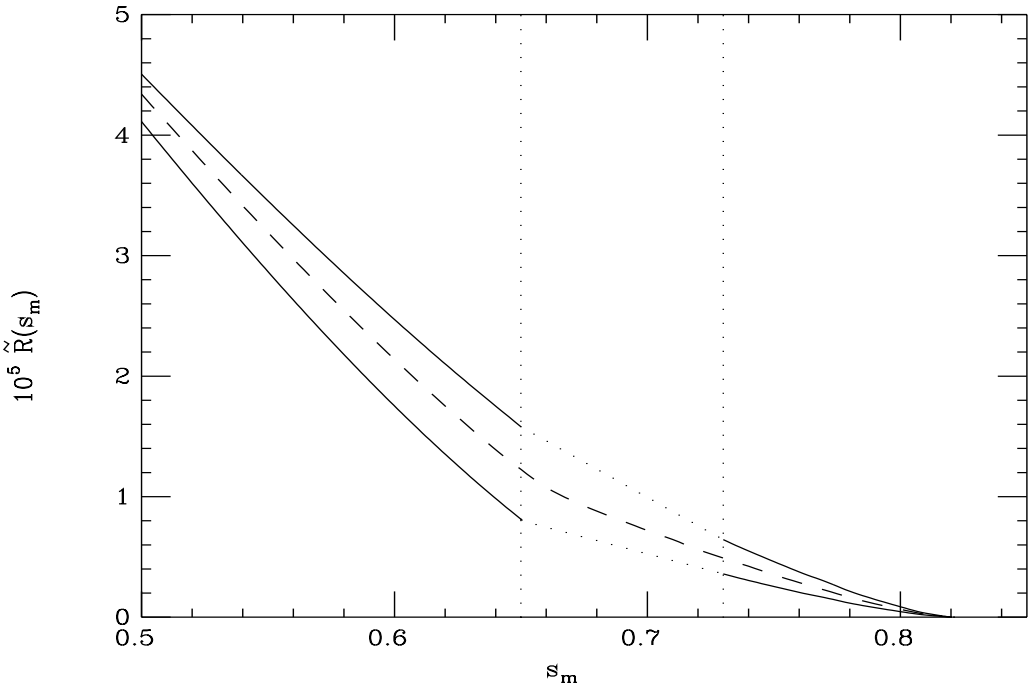

Figure 1: The dilepton invariant mass spectrum $(dB(\bar{B} \to X_s l^+ l^-)/ds_m)/\ B(\bar{B} \to X_c e\nu) \equiv \tilde{R}(s_m)$ as a function of $s_m = q^2/M_B^2$. For $s_m < 0.65$ the NLO partonic calculation, including $1/m_b^2$ effects, is used. There the lower, middle and upper curves correspond to $m_b/\mathrm{GeV} = 4.7$, 4.8 and 4.9, respectively. For $s_m > 0.73$ we show the HHChPT prediction for $\tilde{R}(s_m)$, which is dominated by $\bar{B} \to \bar{K} l^+ l^-$. Lower, middle and upper curve are obtained for $g = 0.4$, 0.5 and 0.6. Linear interpolations between the two regions ($0.65 < s_m < 0.73$) are indicated by dotted lines to guide the eye. The dashed curve illustrates a smooth interpolation using central parameter values. The thresholds for the various exclusive modes occur at $s_m = 0.821$ (K), 0.774 ($K\pi$), 0.728 ($K\pi\pi$), 0.691 ± 0.008 (K^*, $\pm$ half width).

and $s_m > 0.73$, where HHChPT may be used. In this way an essentially model independent description of the entire high-q^2 region $s_m > 0.5$ (above the Ψ' resonance) could be obtained, at least in principle. In practice there are however several sizable uncertainties associated in particular with the HHChPT treatment. The $B^* B\pi$ coupling g is still poorly known. Other uncertainties are related to the values of $|V_{ts}|$ and $\tau(B_d)$ entering (30), but these are less important than the one from g. Also the B meson decay constant f_B introduces some uncertainty.

A further issue is the reliability of chiral perturbation theory in the present case. The kaon mass is not very small with respect to the chiral symmetry breaking scale $\Lambda_\chi \sim 1.2$ GeV. Thus, even in the vicinity of the endpoint, corrections of order 30%–40% can be expected. In the $K\pi$ channel the situation could be even worse, given the presence of the nearby K^*

resonance. However, for a given value of s_m the hadronic invariant mass ranges from M_K to $M_{had}^{max} = M_B(1 - s_m^{1/2}) \simeq 770$ MeV and only near the upper figure the effect of the resonance should be important. Given the above remarks, the result for $\tilde{R}(s_m)$ we have presented should still provide a reasonable estimate. In addition, in view of the kinematical suppression of the $K\pi$ channel, the fact that the region above $s_m = 0.73$ is entirely determined by $\bar{B} \to \bar{K} l^+ l^-$ can be expected to be valid beyond the limitations of chiral perturbation theory, which is useful for further studies.

Systematic improvements are possible by going beyond the lowest order in HHChPT. In [32] chiral logarithmic corrections to the leading result have been investigated within HHChPT for the exclusive mode $\bar{B} \to \bar{K} l^+ l^-$. The corrections were found to be about 40%, which is sizable but still moderate enough for the approach to make sense. A related issue is the question of whether to use f_K instead of f_π, which also goes beyond the leading order of chiral perturbation theory. The calculation of [32] can be considered as a naive estimate of the expected size of the higher-order corrections, but lack of knowledge of the corresponding counterterms makes any precise statement about their exact value difficult. For this reason we have not explicitly included the chiral logarithms in our estimates. The related uncertainty is at least partly included in our variation of the coupling g.

Apart from the differential branching fraction also the forward-backward asymmetry can be studied in HHChPT at large q^2. In this context we note that A_{FB} vanishes identically for the single kaon mode $\bar{B} \to \bar{K} l^+ l^-$. The endpoint of A_{FB} is therefore determined by $\bar{B} \to \bar{K} \pi l^+ l^-$ and occurs at $s_m = (1 - (M_K + M_\pi)/M_B)^2 = 0.774$.

We finally remark that the entire high-q^2 region (defined by $0.5 \leq s_m \leq 0.821$) corresponds to an integrated branching ratio for $\bar{B} \to X_s l^+ l^-$ of about $0.5 \cdot 10^{-6}$ in the Standard Model. Thus, although the dilepton mass spectrum is dropping to zero towards the endpoint, a sizable branching fraction for $\bar{B} \to X_s l^+ l^-$ exists in the region that is characterized by the transition from quark level dynamics to HHChPT. The high-q^2 regime constitutes one of the interesting regions to search for $\bar{B} \to X_s l^+ l^-$ in experiment [35–37]. Attempts to describe this part of the spectrum in a model independent way along the lines proposed in this paper should therefore be useful for the study of rare B decays at future B physics facilities.

5 Other nonperturbative corrections

In addition to higher order terms in the $1/m_b$ expansion, $\bar{B} \to X_s l^+ l^-$ decays are affected by long-distance corrections related to $c\bar{c}$ intermediate states. These originate from the nonperturbative interactions of the $c\bar{c}$ pair in the process $\bar{B} \to X_s c\bar{c} \to X_s l^+ l^-$. If the dilepton invariant mass is close to one of the two narrow $J^{PC} = 1^{--}$ $c\bar{c}$-resonances

($\Psi(3097)$ and $\Psi'(3686)$) this effect is very large and "obscures" the short-distance FCNC process. However, this background can be eliminated by suitable cuts on the dilepton invariant mass. Given the vicinity of the two narrow resonances, two q^2-regions naturally emerge as appropriate for the study of short-distance dynamics: the region below the Ψ and the one above the Ψ'. In the first case it is still necessary to deal with the $c\bar{c}$ rescattering below threshold, whereas in the second case the effect of broader resonances and open charm has to be evaluated.

Nonperturbative contributions generated by $c\bar{c}$ intermediate states have been widely discussed in the literature by means of phenomenological resonance-exchange models [4, 12–14]. These approaches are useful near the main resonance peaks, but their validity outside this region is certainly less reliable. Indeed, the shape of the resonance tails far from the peaks is not under control. Moreover, a double-counting problem is usually posed by the simultaneous use of quark and hadronic degrees of freedom. Within this framework, the only way to avoid double counting is represented by the approach of [12] (KS). Here, in order to take into account charm rescattering, the correction to C_9 induced by $b \to c\bar{c}s$ operators is estimated by means of experimental data on $\sigma(e^+e^- \to c\bar{c}\text{-hadrons})$ using a dispersion relation. To be more specific, the function $h(z,s)$ appearing in (27) is replaced by

$$h(z,s) \longrightarrow h(z,0) + \frac{s}{3} P \int_{s_c}^{\infty} ds' \frac{R_{\rm had}^{c\bar{c}}(s')}{s'(s'-s)} + i\frac{\pi}{3} R_{\rm had}^{c\bar{c}}(s) \,, \tag{50}$$

where $R_{\rm had}^{c\bar{c}}(s) = \sigma(e^+e^- \to c\bar{c})/\sigma(e^+e^- \to \mu^+\mu^-)$ and s_c is the $c\bar{c}$ threshold. This method has also the advantage of including open charm contributions. However, it is exact only in the limit where the $\bar{B} \to X_s c\bar{c}$ transition can be factorized into the product of $\bar{s}b$ and $\bar{c}c$ color-singlet currents (i.e. *non-factorizable* effects are not included). Using this method we have estimated the long-distance corrections to the plot in Figure 1. The effect is quite small, at the level of several percent, essentially negligible for $s_m \gtrsim 0.53$. Below this value the correction exceeds 10% because of the vicinity of the Ψ' peak.

Larger effects from the higher $c\bar{c}$ resonances ($\Psi(3770)$, $\Psi(4040)$, $\Psi(4160)$, $\Psi(4415)$) are obtained when a phenomenological factor $\kappa \approx 2.3$ is introduced to enhance resonance production with respect to the factorization result [38]. This is motivated by the fact that the factorization assumption yields too small values for the $\bar{B} \to J/\Psi X_s$ branching fraction. The validity of such a procedure for estimating the impact of higher resonances in $\bar{B} \to X_s l^+ l^-$ is not entirely clear. Further work on this issue is necessary. In any case the deviations from quark-hadron duality due to resonances are reduced when the $\bar{B} \to X_s l^+ l^-$ spectrum is integrated over a large enough range of q^2.

A more systematic and model-independent way to estimate $c\bar{c}$ long-distance effects far from the resonance region, based on a heavy quark expansion in inverse powers of

the charm-quark mass, has been recently presented in [16] (see also [17]). This approach, originally proposed in [39] to evaluate similar effects in $B \to X_s\gamma$ decays, has the advantage of dealing only with partonic degrees of freedom. In this framework the leading nonperturbative corrections to $R(s)$ turn out to be $\mathcal{O}(\Lambda^2_{QCD}/m_c^2)$. They originate from the effective $\bar{s}b$–photon–gluon vertex (induced by charm loops), where the gluon is soft and couples to the light cloud surrounding the b quark inside the B meson. The corresponding matrix elements can be related to λ_2 and thus are known both in magnitude and in sign. This kind of corrections is complementary to those computed in the KS approach, since they are generated by the charm rescattering in a color-octet state. Since the factorizable corrections vanish for $s \to 0$, as shown by (50), the $\mathcal{O}(\Lambda^2_{QCD}/m_c^2)$ effect is expected to be the dominant long-distance contribution for small values of the dilepton invariant mass. For $s < 0.2$ the relative magnitude of the correction is very small (at the one or two percent level). Higher-order terms become more and more important near the $c\bar{c}$ threshold, where the description in terms of partonic degrees of freedom is clearly inadequate. Using a simple order-of-magnitude estimate of higher-order terms, it has been shown that the leading corrections should provide a reasonable estimate of the effect up to $s = 3m_c^2/m_b^2 \approx 0.26$ ($s_m < 0.21$) [16]. In this region the effect is below 4%. The $\mathcal{O}(\Lambda^2_{QCD}/m_c^2)$ corrections are again very small above the Ψ' peak.

6 Conclusions

Within the framework of the heavy quark expansion we have computed the nonperturbative corrections of $\mathcal{O}(\Lambda^2_{QCD}/m_b^2)$ to the dilepton invariant mass spectrum and the lepton forward-backward asymmetry in $\bar{B} \to X_s l^+ l^-$ decay. Our calculations confirm the results of [14] for these quantities, which were at variance with earlier work [5]. For completeness we have also written down the $\mathcal{O}(\Lambda^2_{QCD}/m_b^2)$ corrections for the lepton left-right asymmetry.

In the main part of our paper we have then focussed on the region of high dilepton invariant mass q^2 (with $q^2 > M^2_{\Psi'}$). This is one of the relevant search regions in experiments looking for $\bar{B} \to X_s l^+ l^-$ and corresponds to an integrated branching ratio of about $0.5 \cdot 10^{-6}$ in the Standard Model. The HQE breaks down for q^2 too close to its maximum value at the endpoint of the dilepton mass spectrum. This is signalled by a manifest divergence of the relative $\mathcal{O}(\Lambda^2_{QCD}/m_b^2)$ corrections in the limit $q^2 \to m_b^2$, as already observed in [14]. We have discussed conceptual aspects of this breakdown of the HQE for $\bar{B} \to X_s l^+ l^-$ and emphasized that it is impossible to remedy the failure of the usual $1/m_b$ expansion at the endpoint by an all-orders resummation, in contrast to the case of e.g. the photon energy spectrum in $\bar{B} \to X_s\gamma$. We were therefore led to consider an al-

ternative, model independent approach to the endpoint region using HHChPT, which is in principle well suited in this kinematical regime. For this purpose we have formulated, at NLO in QCD, an effective Hamiltonian adapted to the endpoint region. This Hamiltonian is a variant of the standard Hamiltonian for $b \to s l^+ l^-$ transitions and serves as the basis for calculating the relevant exclusive channels in the vicinity of $q^2 = (M_B - M_K)^2$ within HHChPT. We explicitly considered the modes $\bar{B} \to \bar{K} l^+ l^-$ and $\bar{B} \to \bar{K} \pi l^+ l^-$ and demonstrated that the latter is completely negligible in the kinematical region of interest. To obtain a complete description of the high-q^2 spectrum, an interpolation between the HHChPT regime and the region of validity of the heavy quark expansion has been suggested. At present there are still limitations in accuracy from uncertainties in the value of m_b and, particularly, in the poorly known HHChPT parameter g as well as due to neglected higher order terms in the chiral expansion. However, the approach is essentially model independent and systematic improvements can in principle be made.

Acknowledgments

We thank Stefano Bellucci, Martin Beneke and Gilberto Colangelo for interesting discussions and a critical reading of the manuscript.

References

[1] W.S. Hou, R.I. Willey and A. Soni, Phys. Rev. Lett. **58**, 1608 (1987).

[2] B. Grinstein, M.J. Savage and M.B. Wise, Nucl. Phys. **B319**, 271 (1989).

[3] W. Jaus and D. Wyler, Phys. Rev. **D41**, 3405 (1990).

[4] A. Ali, T. Mannel and T. Morozumi, Phys. Lett. **B273**, 505 (1991).

[5] A.F. Falk, M. Luke and M.J. Savage, Phys. Rev. **D49**, 3367 (1994).

[6] A. Ali, G.F. Giudice and T. Mannel, Z. Phys. **C67**, 417 (1995).

[7] M. Misiak, Nucl. Phys. **B393**, 23 (1993); erratum ibid. **B439**, 461 (1995).

[8] A.J. Buras and M. Münz, Phys. Rev. **D52**, 186 (1995).

[9] J.L. Hewett, Phys. Rev. **D53**, 4964 (1996).

[10] G. Buchalla, G. Burdman, C.T. Hill and D. Kominis, Phys. Rev. **D53**, 5185 (1996).

[11] P. Cho, M. Misiak and D. Wyler, Phys. Rev. **D54**, 3329 (1996).

[12] F. Krüger and L.M. Sehgal, Phys. Lett. **B380**, 199 (1996).

[13] M.R. Ahmady, Phys. Rev. **D53**, 2843 (1996); C.-D. Lü and D.-X. Zhang, Phys. Lett. **B397**, 279 (1997).

[14] A. Ali, G. Hiller, L.T. Handoko and T. Morozumi, Phys. Rev. **D55**, 4105 (1997).

[15] J.L. Hewett and J.D. Wells, Phys. Rev. **D55**, 5549 (1997).

[16] G. Buchalla, G. Isidori and S.J. Rey, SLAC-PUB-7448, hep-ph/9705253, to appear in Nucl. Phys. B.

[17] J.-W. Chen, G. Rupak and M.J. Savage, DOE/ER/41014-10-N97, hep-ph/9705219.

[18] A. Masiero and L. Silvestrini, TUM-HEP-291-97, hep-ph/9709244.

[19] G. Burdman, hep-ph/9710550.

[20] G. Buchalla, A.J. Buras and M.E. Lautenbacher, Rev. Mod. Phys. **68**, 1125 (1996).

[21] O. Bär and N. Pott, Phys. Rev. **D55**, 1684 (1997).

[22] D.S. Liu and R. Delbourgo, Phys. Rev. **D53**, 548 (1996).

[23] A.V. Manohar and M.B. Wise, Phys. Rev. **D49**, 1310 (1994).

[24] I.I. Bigi, M.A. Shifman, N.G. Uraltsev and A.I. Vainshtein, Phys. Rev. Lett. **71**, 496 (1993).

[25] I.I. Bigi, M.A. Shifman, N.G. Uraltsev and A.I. Vainshtein, Int. J. Mod. Phys. **A9**, 2467 (1994).

[26] T. Mannel and M. Neubert, Phys. Rev. **D50**, 2037 (1994).

[27] M. Neubert, Phys. Rev. **D49**, 3392 (1994).

[28] M. Neubert, Phys. Rev. **D49**, 4623 (1994).

[29] M.B. Wise, Phys. Rev. **D45**, R2188 (1992).

[30] G. Burdman and J.F. Donoghue, Phys. Lett. **B280**, 287 (1992).

[31] P. Colangelo et al., Phys. Rev. **D53**, 3672 (1996).

[32] A.F. Falk and B. Grinstein, Nucl. Phys. **B416**, 771 (1994).

[33] R. Casalbuoni et al., Phys. Rept. **281**, 145 (1997).

[34] C.L.Y. Lee, M. Lu and M.B. Wise, Phys. Rev. **D46**, 5040 (1992).

[35] C. Albajar et al. (UA1 collaboration), Phys. Lett. **B262**, 163 (1991).

[36] S. Glenn et al. (CLEO collaboration), CLNS-97-1514, hep-ex/9710003.

[37] B. Abbott et al. (D0 collaboration), hep-ex/9801027.

[38] Z. Ligeti, I.W. Stewart and M.B. Wise, hep-ph/9711248.

[39] M.B. Voloshin, Phys. Lett. **B397**, 275 (1997); A. Khodjamirian, R. Rückl, G. Stoll and D. Wyler, WUE-ITP-97-001, hep-ph/9702318.